

Water–Benzene Interactions: An Effective Fragment Potential and Correlated Quantum Chemistry Study[†]

Lyudmila V. Slipchenko[‡] and Mark S. Gordon*

Department of Chemistry and Ames Laboratory, Iowa State University, Ames, Iowa 50011

Received: October 6, 2008; Revised Manuscript Received: November 5, 2008

Structures and binding in small water–benzene complexes (1–8 water molecules and 1–2 benzene molecules) are studied using the general effective fragment potential (EFP) method. The lowest energy conformers of the clusters were found using a Monte Carlo technique. The binding energies in the smallest clusters (dimers, trimers, and tetramers) were also evaluated with second order perturbation theory (MP2) and coupled cluster theory (CCSD(T)). The EFP method accurately predicts structures and binding energies in the water–benzene complexes. Benzene is polarizable and consequently participates in hydrogen bond networking of water. Since the water–benzene interactions are only slightly weaker than water–water interactions, structures with different numbers of water–water, benzene–water, and benzene–benzene bonds often have very similar binding energies. This is a challenge for computational methods.

I. Introduction

Interaction of aromatic molecules with solvents is of fundamental interest since these interactions are common in biosystems.^{1–4} The simplest systems of this type, small benzene–water complexes, have attracted both experimental and theoretical attention.^{5–20} In a series of papers, Zwier and co-workers^{7–12} presented accurate IR data on (benzene)_{1–2}–(water)_{1–8} complexes. Accurate assignments of the spectral features of these clusters would provide unambiguous information on their structures. However, accurate theoretical investigation of these clusters is challenging, because both an extensive basis set with diffuse functions and a high level of dynamical correlation are required for their accurate treatment.⁵ Moreover, as will be shown in this study, binding in water–benzene complexes has a complicated nature, because electrostatic interactions specific to hydrogen-bonded water, π – π type interactions common to benzenes, and π –H benzene–water forces all play important roles. Thus, to provide an accurate analysis of these systems, the theoretical method should possess comparably accurate descriptions of the different contributions to the binding energies, such as Coulomb, induction, and dispersion interactions. It is recognized that second order perturbation theory, MP2,²¹ tends to *overestimate* dispersion forces, whereas density functional theory (DFT) methods with the most commonly employed functionals typically do not describe dispersion well.

This study investigates the structures and bonding in small water–benzene complexes by means of the general effective fragment potential (EFP) method.²² EFP is a first-principles-based model potential method in which all of the parameters are derived from first principles electronic structure calculations. Currently, the EFP interaction energy includes Coulomb, induction, dispersion, exchange repulsion, and charge-transfer terms (the latter was omitted in the current study). Previous studies have demonstrated that the EFP method accurately

describes, for example, chemical reactions in water,^{23,24} mixing of water and methanol,²⁵ and interactions in the benzene dimer and its derivatives.^{26,27} The present contribution considers water–benzene interactions, which are prototypical for biochemistry. The objectives are, first, to benchmark the performance of the EFP method against accurate *ab initio* methods, MP2 and CCSD(T)²⁸ [the coupled cluster approach with single, double and perturbative triple excitations] for small water–benzene complexes (dimers, trimers, and tetramers), and second, to perform an independent EFP study for larger complexes (up to eight waters and two benzenes). Questions targeted in this work are as follows: (i) What is the nature of the binding forces between water and benzene? (ii) If and how does attachment of benzene molecules affect the structure of water clusters? (iii) Do water–benzene complexes show cooperative behavior? (iv) In complexes with two benzenes, do the benzene molecules become separated by waters or stay together, and how does this tendency change as a function of the cluster size.

The structure of this paper is as follows: the next section describes the computational procedure. Section III presents the main results. Conclusions are drawn in section IV.

II. Computational Details

All calculations were performed using the GAMESS (General Atomic and Molecular Electronic Structure System) electronic structure package.^{29,30}

EFP is a model potential method in which all of the parameters are derived from first principles electronic structure calculations. At present, the EFP interaction energy is a sum of five terms:²²

$$E = E_{\text{coul}} + E_{\text{ind}} + E_{\text{exrep}} + E_{\text{disp}} + E_{\text{ct}} \quad (1)$$

E_{coul} refers to the Coulomb portion of the electrostatic interaction. This term is obtained using the distributed multipolar expansion introduced by Stone,³¹ with the expansion carried out through octopoles. E_{ind} is the induction or polarization part of the electrostatic interaction. This term is represented by the interaction of the induced dipole on one fragment with the electrostatic field on another fragment, expressed in terms of

[†] Part of the “Max Wolfsberg Festschrift”.

* Corresponding author.

[‡] Current address: Department of Chemistry, Purdue University, West Lafayette, IN 47907.

TABLE 1: Intermolecular Distances (angstroms) and Binding Energies (kcal/mol) in the W1B1a Water–Benzene Dimer

method	ref	R_e^a	D_e^b	D_0
MP2/aVTZ	Feller ⁵	3.21	−4.0 (−3.1)	−3.0(−2.1) ^c
CCSD(T)/aVTZ	Feller ⁵		−3.9	−2.9 ^c
Est. MP2/CBS	Feller ⁵		−3.9 ± 0.2	−2.9 ± 0.2 ^c
EFP	this work	3.38	−3.9	−2.9
expt	Gotch, Zwier ⁷	3.32		−1.63 to −2.78
	Suzuki et al. ²⁰	3.35		
	Gutowsky et al. ¹⁸	3.33		
	Cheng et al. ¹⁶			−2.25 ± 0.28
	Courty et al. ¹⁷			−2.44 ± 0.09

^a Distance between the water and benzene centers of mass. ^b Values in parentheses correspond to counterpoise-corrected (CP) binding energies. ^c Using estimated zero-point vibrational energy from ref 5.

TABLE 2: Electronic Binding Energies (kcal/mol) in the W1B1a Water–Benzene Dimer

basis	geometry	MP2			CCSD(T)		
		no CP	CP	av	no CP	CP	av
cc-pVDZ	EFP ^a	−3.6	−1.9	−2.8	−3.3	−1.7	−2.5
cc-pVTZ	EFP ^a	−4.0	−2.7	−3.4	−3.7	−2.4	−3.1
cc-pVQZ	EFP ^a	−3.8	−3.0	−3.4			
cc-pV5Z	EFP ^a	−3.5	−3.2	−3.3	−3.1 ^c	−2.9 ^c	−3.0 ^c
cc-pV∞Z(3-4)	EFP ^a	−3.9	−3.3	−3.6			
cc-pV∞Z(4-5)	EFP ^a	−3.4	−3.3	−3.4	−3.1 ^c	−3.0 ^c	−3.1 ^c
aug'-cc-pVDZ ^b	EFP ^a	−3.7	−2.3	−3.0	−3.5	−2.1	−2.8
aug'-cc-pVTZ ^b	EFP ^a	−3.7	−3.0	−3.3			
aug'-cc-pVQZ ^b	EFP ^a	−3.4	−3.1	−3.3	−3.2 ^c	−2.9 ^c	−3.0 ^c
aug'-cc-pV∞Z(2-3)	EFP ^a	−3.8	−3.3	−3.6			
aug'-cc-pV∞Z(3-4)	EFP ^a	−3.2	−3.2	−3.2	−3.1	3.0	−3.0
aug'-cc-pVDZ ^b	MP2 ^d	−4.1	−2.4	−3.3	−3.9	−2.1	−3.0
aug'-cc-pVTZ ^b	MP2 ^d	−3.9	−3.3	−3.6	−3.7 ^c	−3.0 ^c	−3.3
aug'-cc-pVQZ ^b	MP2 ^d	−3.6	−3.4	−3.5	−3.4 ^c	−3.2 ^c	−3.3 ^c
aug'-cc-pV∞Z(2-3)	MP2 ^d	−4.0	−3.7	−3.9			
aug'-cc-pV∞Z(3-4)	MP2 ^d	−3.5	−3.6	−3.5	−3.2	−3.3	−3.2

^a Calculated at EFP equilibrium geometry. ^b Basis sets as described in text. ^c Extrapolated using energy additivity formula (see text). ^d Calculated at the MP2/aug'-cc-pVDZ equilibrium geometry.

the dipole polarizability. The molecular polarizability is expressed as a tensor sum of localized molecular orbital (LMO) polarizabilities. That is, the number of polarizability points is equal to the number of bonds and lone pairs in the molecule. These induced dipoles are iterated to self-consistency, so some many body effects are included.

The exchange repulsion E_{exrep} is derived as an expansion in the intermolecular overlap, truncated at the quadratic term.³² This term does require that each EFP carries a basis set, and the smallest recommended basis set is 6-31++G(d,p)³³ for acceptable results. Since the basis set is used only to calculate overlap integrals, the computation is very fast and quite large basis sets are realistic. The dispersion interaction can be expressed as the familiar inverse R expansion,

$$E_{\text{disp}} = \sum_n C_n R^{-n} \quad (2)$$

The coefficients C_n may be derived from the (imaginary) frequency dependent polarizabilities summed over the entire frequency range.^{34,35} If one employs only dipole polarizabilities the dispersion expansion is truncated at the leading term, with $n = 6$. In the current EFP code, an estimate is used for the $n = 8$ term, in addition to the explicitly derived $n = 6$ term. Rather than express a molecular C_6 as a sum over atomic interaction terms, the EFP dispersion is expressed in terms of LMO-LMO interactions.

The charge transfer interaction E_{ct} is derived using a supermolecule approach, in which the occupied valence molecular orbitals on one fragment interact with the virtual orbitals on

another fragment. This leads to significant energy lowering in *ab initio* calculations on ionic or highly polar species when incomplete basis sets are employed. An approximate formula³⁶ is obtained in canonical orbitals from Hartree–Fock calculations of independent molecules and uses a multipolar expansion (through quadrupoles) of the molecular electrostatic potentials. The charge-transfer interactions were omitted in this study.

EFP parameters for water and benzene were obtained with the 6-311++G(3df,2p)^{37–39} basis set. The MP2/aug-cc-pVTZ^{40,41} geometry from ref 42 was used for the benzene monomer. The geometry of the water monomer was chosen to have bond lengths of 0.9468 Å and bond angle of 106.70°, to be consistent with previous EFP studies of water.⁴³ Electrostatic parameters for both water and benzene were obtained using the numerical distributed multipolar analysis (DMA), with high-order electrostatic screening.²⁶ Additionally, polarization interactions were screened using damping functions for polarization,⁴⁴ with damping parameters at all centers set to 1.5. To find the lowest energy structures, multiple Monte-Carlo/simulated annealing (MC/SA)⁴⁵ simulations were performed for clusters of each size. To ensure better sampling of the conformational space, these simulations were initialized from different starting geometries, and were run with various starting and final temperatures in the range 100–20000 K. Each structure was assigned a unique name; e.g., W1B1a means that the complex consists of one water molecule (W1) and one benzene molecule (B1) and is the lowest in energy (a).

The basis sets used for the MP2 calculations on the lowest-energy minimum of the water–benzene dimer (W1B1a) were

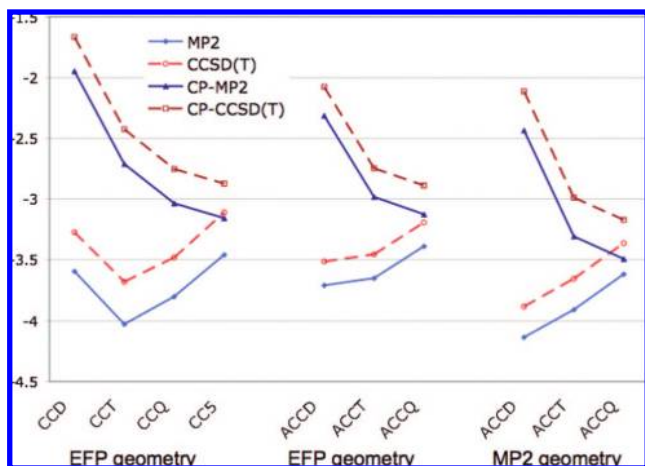


Figure 1. Binding energies (kcal/mol) in the water–benzene dimer. CCD, CCT, etc. correspond to the cc-pVDZ, cc-pVTZ, etc. basis sets; ACCD, ACCT, ACCQ correspond to the aug'-cc-pVDZ, aug'-cc-pVTZ, aug'-cc-pVQZ basis sets (see text for details). The left and middle panels show the data obtained at the EFP geometry; the right panel shows the data obtained at the MP2/aug'-cc-pVDZ geometry of the dimer. The blue and dark-blue curves represent the MP2 noncorrected and CP-corrected data, respectively; the red and dark-red curves show the CCSD(T) noncorrected and CP-corrected data, respectively. The CCSD(T) points in the CCQ, CC5, ACCT, and ACCQ basis sets are estimated using eq 3.

the correlation-consistent basis sets: cc-pVDZ, cc-pVTZ, cc-pVQZ, cc-pV5Z (with the h functions omitted),⁴⁰ and their augmented (by diffuse functions) analogs, aug'-cc-pVDZ, aug'-cc-pVTZ, and aug'-cc-pVQZ.⁴¹ The prime in aug'-cc-pVDZ means that only s diffuse functions on H and s and p diffuse functions on C and O were added. In aug'-cc-pVTZ and aug'-cc-pVQZ, s, p diffuse functions on H and s, p, d diffuse functions on heavy atoms were used. CCSD(T) calculations on W1B1a were performed using the cc-pVDZ, cc-pVTZ, and aug'-cc-pVDZ basis sets. For the other clusters, MP2/aug'-cc-pVDZ, MP2/aug'-cc-pVTZ, and CCSD(T)/aug'-cc-pVDZ energies were obtained, both with and without counterpoise-corrections (CP). The CCSD(T) energies using the largest basis sets (cc-pV5Z and aug'-cc-pVQZ for W1B1a, and aug'-cc-pVTZ for the other clusters) were estimated by using the energy additivity scheme.^{46–49}

$$E_{CCSD(T)}^{big} = E_{CCSD(T)}^{small} + (E_{MP2}^{big} - E_{MP2}^{small}) \quad (3)$$

where *big* and *small* correspond to the bigger and smaller basis sets, e.g., cc-pV5Z and cc-pVTZ, respectively. The complete basis set (CBS) limits for the MP2 binding energies in the water–benzene dimer were estimated using the following formula:^{50–54}

$$E_{CBS}^{corr} = E_X^{corr} - AX^{-3} \quad (4)$$

where *X* is the order of the pVXZ correlation-consistent basis set. E^{corr} is the correlation energy, i.e., the difference between the MP2 and Hartree–Fock (HF) total energies. In order to compare the quality of this extrapolation scheme for augmented and nonaugmented basis sets, $X = 3, 4$ and $X = 4, 5$ were used for extrapolations with the cc-pVXZ series, and $X = 2, 3$ and $X = 3, 4$ were used for the aug'-cc-pVXZ series. The uncorrelated HF energies were not extrapolated to the CBS limit. Instead, the energies in the largest basis used in a particular CBS scheme were employed.^{50–54} CBS values for CCSD(T) were estimated using a combination of eqs 3 and 4.

	electrost.	exch.-repulsion	induction	dispers.	total binding	total+ Δ ZPE
	-8.6	5.3	-1.0	-0.9	-5.1	-2.6
	-3.8	2.3	-0.6	-1.8	-3.9	-2.9
	-3.9	3.2	-0.4	-1.4	-2.6	-1.6
	-0.1	2.9	-0.3	-4.9	-2.4	-2.0
	-1.8	2.4	-0.2	-3.2	-2.9	-2.4

Figure 2. Interaction energy components (kcal/mol) in the water dimer, benzene dimers, and water–benzene dimers.

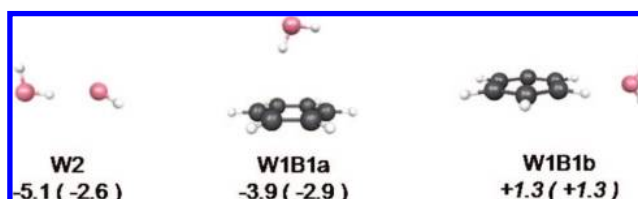


Figure 3. EFP dimer structures. Total interaction energies (kcal/mol) and ZPE corrected values (in parentheses) are given for the lowest energy conformer; energies relative to the lowest energy structure are given for other complexes.

Most MP2 and CCSD(T) calculations were performed at the EFP geometries of the clusters, determined via the Monte Carlo simulations, with the exception of the W1B1a and W3B1 complexes, where an additional geometry optimization was performed at the MP2/aug'-cc-pVDZ level of theory. Geometries of benzene and water were maintained fixed in this MP2 optimization of W1B1a and were allowed to relax in the optimization of the W3B1 complexes; the latter were followed by full vibrational frequency analysis. The EFP and MP2 geometries of water–benzene clusters can be found in the Supporting Information.

III. Results and Discussion

Table 1 summarizes the experimental and theoretical intermolecular distances and binding energies for the lowest energy structure of the water–benzene dimer. The experimental values of the intermolecular distances (determined as the distance between the centers of mass in water and benzene) are 3.32–3.35 Å. MP2 underestimates these values by more than 0.1 Å, whereas EFP overestimates them by about 0.05 Å. There is considerable variation in the measured water–benzene dimer binding energies, with a range from 1.63 to 2.78 kcal/mol. Calculated binding energies dramatically depend on the method and basis set used (see also Table 2 and Figure 1). Feller concluded that the MP2 electronic binding energy in the estimated complete basis set (CBS) limit is 3.9 ± 0.2 kcal/mol; the corresponding value including vibrational zero-point energy (ZPE) is 2.9 ± 0.2 kcal/mol.⁵ The EFP water–benzene binding energy is 3.9 kcal/mol. Combined with the EFP ZPE, this becomes 2.9 kcal/mol, in very good agreement with the MP2/CBS limit and higher than the experimental values by about 0.5 kcal/mol.

Table 2 summarizes *ab initio* binding energies for W1B1a calculated in this work. The graphical representation of these data is shown in Figure 1. In order to estimate the importance

TABLE 3: Electronic Interaction Energies (kcal/mol) in W1B1b, W2B1, and W1B2a Clusters^a

cluster	basis	MP2			CCSD(T)			EFP
		no CP	CP	av	no CP	CP	av	
W1B1b	aug'-cc-pVDZ	-2.3	-0.6	-1.5	-2.4	-0.6	-1.5	-2.6
	aug'-cc-pVTZ	-1.6	-1.2	-1.4	-1.6 ^b	-1.1 ^b	-1.4 ^b	
W2B1	aug'-cc-pVDZ	-11.5	-7.8	-9.7	-11.2	-7.3	-9.2	-10.9
	aug'-cc-pVTZ	-10.8	-9.4	-10.1	-10.4 ^b	-8.9 ^b	-9.7 ^b	
W1B2a	aug'-cc-pVDZ	-10.9	-6.3	-8.6	-9.9	-5.1	-7.5	-8.8
	aug'-cc-pVTZ	-9.8	-8.1	-9.0	-8.8 ^b	-7.0 ^b	-7.9 ^b	

^a Calculated at the EFP equilibrium geometries. Basis sets as described in text. ^b Estimated using energy additivity formula, see text.

TABLE 4: Electronic Interaction Energies (kcal/mol) in W3B1 Clusters^a

cluster	basis	MP2			CCSD(T)			EFP
		no CP	CP	av	no CP	CP	av	
W3B1a	aug'-cc-pVDZ ^b	-20.7	-14.1	-17.4	-20.2	-13.3	-16.8	-20.7 (-13.6)
	aug'-cc-pVTZ ^b	-19.0	-16.8	-17.9	-18.6 ^d	-16.0 ^d	-17.3 ^d	
W3B1b	aug'-cc-pVDZ ^c	-22.2 (-16.2)						
	aug'-cc-pVDZ ^b	-21.4	-15.2	-18.3	-21.1	-14.6	-17.8	-19.6 (-12.6)
	aug'-cc-pVTZ ^b	-20.0	-17.9	-18.9	-19.7 ^d	-17.3 ^d	-18.5 ^d	
W3B1c	aug'-cc-pVDZ ^c	-22.9 (-16.4)						
	aug'-cc-pVDZ ^b	-20.8	-14.9	-17.8	-20.5	-14.3	-17.4	-19.4 (-12.5)
	aug'-cc-pVTZ ^b	-19.3	-17.3	-18.3	-19.0 ^d	-16.7 ^d	-17.9 ^d	
	aug'-cc-pVDZ ^c	-22.4 (-16.0)						

^a Basis sets as described in text. Values in parentheses are ZPE corrected. ^b Calculated at the EFP equilibrium geometries. ^c Calculated at the MP2/aug'-cc-pVDZ equilibrium geometry without CP correction. ^d Estimated using energy additivity formula, see text.

TABLE 5: Electronic Interaction Energies (kcal/mol) in W2B2 Clusters^a

cluster	basis	MP2			CCSD(T)			EFP
		no CP	CP	ave	no CP	CP	av	
W2B2a	aug'-cc-pVDZ	-18.6	-12.5	-15.5	-17.5	-11.2	14.3	-17.3
	aug'-cc-pVTZ	-16.7	-14.2	-15.5	-15.6 ^b	-13.0 ^b	-14.3 ^b	
W2B2b	aug'-cc-pVDZ	-15.4	-9.3	-12.4	-14.6	-8.3	11.5	-16.0
	aug'-cc-pVTZ	-13.4	-11.2	-12.3	-12.6 ^b	-10.1 ^b	-11.4 ^b	
W2B2c	aug'-cc-pVDZ	-16.0	-10.3	-13.2	-15.4	-9.6	-12.5	-14.7
	aug'-cc-pVTZ	-14.2	-12.1	-13.2	-13.7 ^b	-11.4 ^b	-12.6 ^b	

^a Calculated at the EFP equilibrium geometries. Basis sets as described in text. ^b Estimated using energy additivity formula, see text.

of the diffuse basis functions, a series of calculations in both the cc-pVXZ and aug'-cc-pVXZ families of bases was performed. These data were obtained at the EFP equilibrium geometry. Additionally, calculations in the aug'-cc-pVXZ bases were performed at the MP2/aug'-cc-pVDZ equilibrium geometry of the dimer, in order to estimate variations in the binding energies upon slight modifications of a chosen dimer geometry.

For each series of calculations, the CBS values for MP2 and CCSD(T) were also obtained using Eq. 4. As expected, the binding energies in the cc-pVDZ basis set are not in good agreement with other cc-pVXZ values. So, cc-pVDZ should not be used in energy approximation schemes. Therefore, basis sets with $X = 3, 4$ and $X = 4, 5$ were used for extrapolations in the cc-pVXZ series, and $X = 2, 3$ and $X = 3, 4$ were used in the aug'-cc-pVXZ series. It is clear from Table 2 that the extrapolations using smaller basis sets, i.e., $X = 3, 4$ in the cc-pVXZ series and $X = 2, 3$ in the aug'-cc-pVXZ series, do not provide sufficiently accurate CBS values. For example, the cc-pV ∞ Z(3-4) CBS limit differs from the cc-pV ∞ Z(4-5) value by more than 0.4 kcal/mol. Subsequent discussions will mainly refer to the results of extrapolations using the two largest bases sets.

For the largest basis sets used, cc-pV5Z and aug'-cc-pVQZ, the MP2 binding energies have similar values: -3.4/-3.5 kcal/mol for the noncorrected calculations and -3.1/-3.2 kcal/mol for the CP-corrected ones. The corresponding CBS values in the two series of bases are -3.3/-3.4 and -3.2 kcal/mol in

noncorrected and CP-corrected calculations, respectively. The difference between the noncorrected and CP-corrected values in the CBS limit is less than 0.1 kcal/mol. The CCSD(T) binding energies in the largest basis sets range from -2.9 to -3.2 kcal/mol and converge to -3.03 ± 0.05 kcal/mol at the CBS limit. It was noted in ref 5 that basis set superposition errors (BSSE) can be non-negligible (about 0.2 kcal/mol) even in the cc-pV5Z and aug'-cc-pVQZ bases. For the aug'-cc-pVTZ basis, with which the MP2 and CCSD(T) calculations for all other water–benzene complexes were performed, the BSSE errors are ~ 0.2 –0.5 kcal/mol. As a computationally less demanding way to estimate the complete basis set limit, the average between the CP-corrected and noncorrected values in each basis set were calculated. These averaged values in the aug'-cc-pVTZ differ only by 0.1 kcal/mol from the corresponding CBS limits. This may be true for other clusters as well.⁵⁵

In the aug'-cc-pVQZ basis set, the MP2 and CCSD(T) binding energies calculated at the MP2/aug'-cc-pVDZ equilibrium geometry are about 0.2 kcal/mol larger than those calculated at the EFP geometry, because MP2, and probably CCSD(T), favors the tighter MP2 geometry over the looser EFP one. Nonetheless, the effect of using the EFP instead of MP2 geometry is relatively minor and is smaller than the effect due to the incompleteness of the basis set in the MP2 and CCSD(T) calculations.

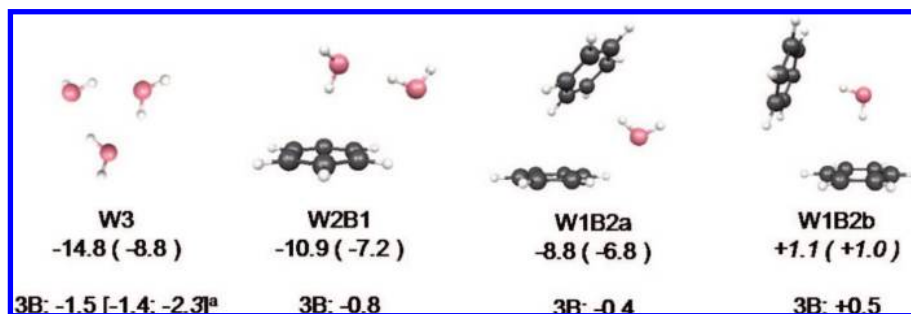


Figure 4. EFP structures of trimers. See Figure 3 for notations. EFP [HF; MP2] three-body energies (3B) in kcal/mol are also shown. HF and MP2 3-body energies for the water trimer are from ref 59.

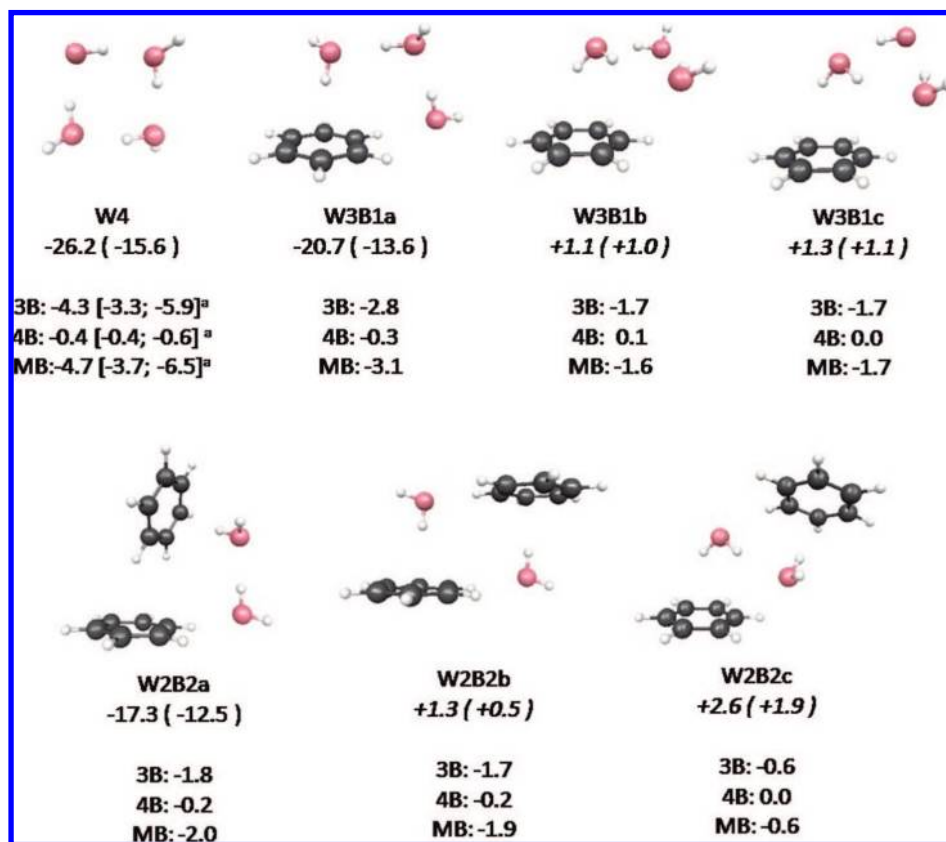


Figure 5. EFP structures of tetramers. See Figure 3 for notations. EFP [HF; MP2] three-body (3B), four-body (4B), and total many-body (MB) energies in kcal/mol are also shown. ^aHF and MP2 many-body energies for water tetramer are from ref 59.

TABLE 6: Interaction Energy Components (kcal/mol) in Water–Benzene Trimers and Tetramers

	Coulomb	ex.-rep	induction	dispersion.	total	total + ZPE
W3	-23.4	15.5	-4.2	-2.8	-14.8	-8.8
W2B1	-14.0	9.8	-2.7	-4.0	-10.9	-7.2
W1B2a	-8.0	7.2	-1.5	-6.5	-8.7	-6.8
W1B2b	-6.7	4.8	-0.8	-5.0	-7.6	-5.7
W4	-43.7	32.6	-10.6	-4.5	-26.2	-15.6
W3B1a	-29.8	22.5	-7.1	-6.3	-20.7	-13.6
W3B1b	-27.8	19.4	-5.0	-6.3	-19.6	-12.6
W3B1c	-27.5	18.8	-4.9	-5.8	-19.4	-12.5
W2B2a	-21.1	17.1	-4.7	-8.5	-17.3	-12.5
W2B2b	-17.9	14.6	-4.4	-8.3	-16.0	-11.9
W2B2c	-16.6	11.8	-2.7	-7.2	-14.7	-10.6

The binding energies obtained in the present work are slightly lower than those reported in ref 5; however, when augmented by the ZPEs, they agree better with the experimental data.

Figure 2 compares binding in the water dimer and benzene dimer with that in the water–benzene dimer. The energy

components were calculated using the EFP method, at the EFP equilibrium geometries for each dimer. It is well-known that the dominant contribution to binding in the water dimer is the electrostatic interaction (-8.6 kcal/mol), whereas the polarization and dispersion interactions are almost 10 times weaker. To the contrary, binding in the parallel-displaced benzene dimer is dominated by dispersion interactions (-4.9 kcal/mol). The T-shaped benzene dimer has significant contributions from both the dispersion and electrostatic interactions; not surprisingly, this is also true for the benzene–water dimer structures. It is also informative to compare the total binding energies of the dimers shown in Figure 2. The water dimer is the most strongly bound, the benzene dimers have the weakest interaction energies, and the water–benzene dimer is in between these two. However, ZPE corrections have an important impact on the relative binding energies. The ZPE-corrected values result in the striking observation that the spread in binding energies is much smaller. Thus, the low miscibility of benzene in water (1.69 ± 0.13

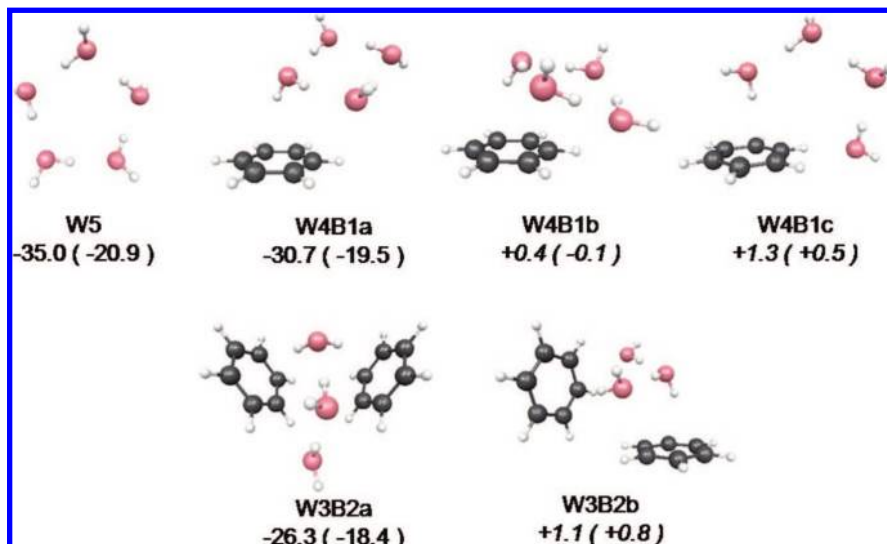


Figure 6. EFP structures of pentamers. See Figure 3 for notations.

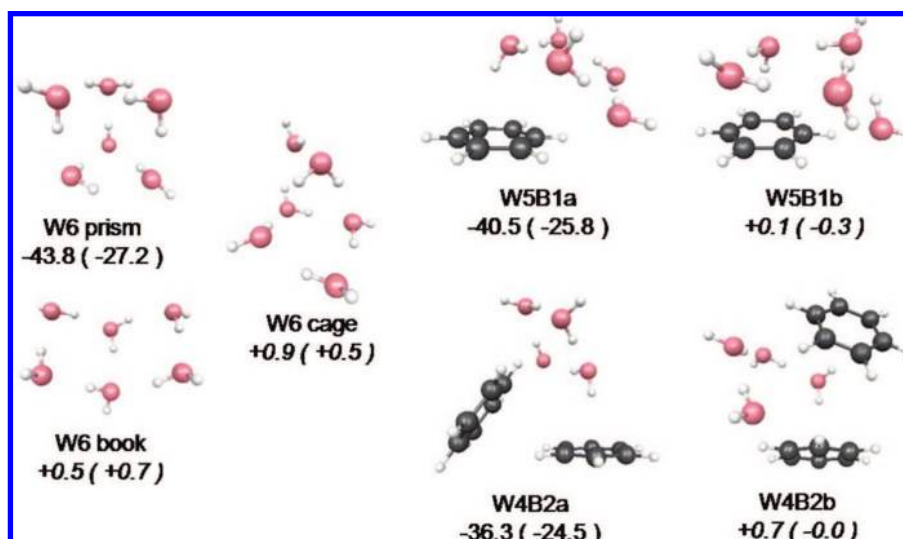


Figure 7. EFP structures of hexamers. See Figure 3 for notations.

g/L^{56–58}) may be due to an unfavorable entropy, rather than enthalpy, contribution.

Figures 3–11 present the lowest energy structures of the water–benzene clusters. The clusters are grouped by the total number of molecules in each cluster, rather than the number of water molecules. EFP classical and ZPE-corrected interaction energies are given below each structure. The MP2, CCSD(T), and EFP binding energies for the global minima W1B1, W2B1, and W1B2 are summarized in Table 3; the W3B1 results are presented in Table 4, and the W2B2 energies are given in Table 5. Generally, these figures and tables illustrate that (i) the water–benzene interactions have a complicated nature, and benzene can serve both as an H-bond donor and acceptor; (ii) water–benzene complexes may experience significant many-body effects which often determine the relative stability of isomers; (iii) because water–water and benzene–water interactions have similar magnitudes, there is competition between structures with different numbers of water–water, benzene–water, and benzene–benzene hydrogen bonds; (iv) in clusters with two benzenes, the relative energies of the structures with separated and directly interacting benzenes are very similar, so that no conclusion can be reached regarding the preference for structures of either type. Moreover, (v) the water–benzene complexes

exhibit strong basis set and correlation effects, and their accurate description by *ab initio* methods is challenging; and (vi) the EFP approach provides an accurate description of structures and interaction energies in water–benzene complexes, with slight discrepancies being observed in the W3B1 and W2B2 complexes. In the following pages these topics will be discussed in more detail.

It is intriguing to trace the patterns by which the benzene molecules build into the water–cluster network. As illustrated in Figure 3, benzene can serve both as a hydrogen bond donor and acceptor. In the global minimum W1B1a, the negatively charged benzene π -cloud donates electron density to a water hydrogen. So, benzene acts as a hydrogen bond acceptor. In the most favorable orientation for this hydrogen bond the water sits on top of the benzene ring, with one of its hydrogens pointing toward the ring. In W1B1b, the water oxygen lone pairs interact with two hydrogens of the benzene ring, so the benzene acts as a hydrogen donor in the hydrogen bond to water. This interaction is strongest when the water is in the same plane as the benzene. As will be discussed later, all of the larger water–benzene clusters are dominated by these two types of water–benzene interactions.

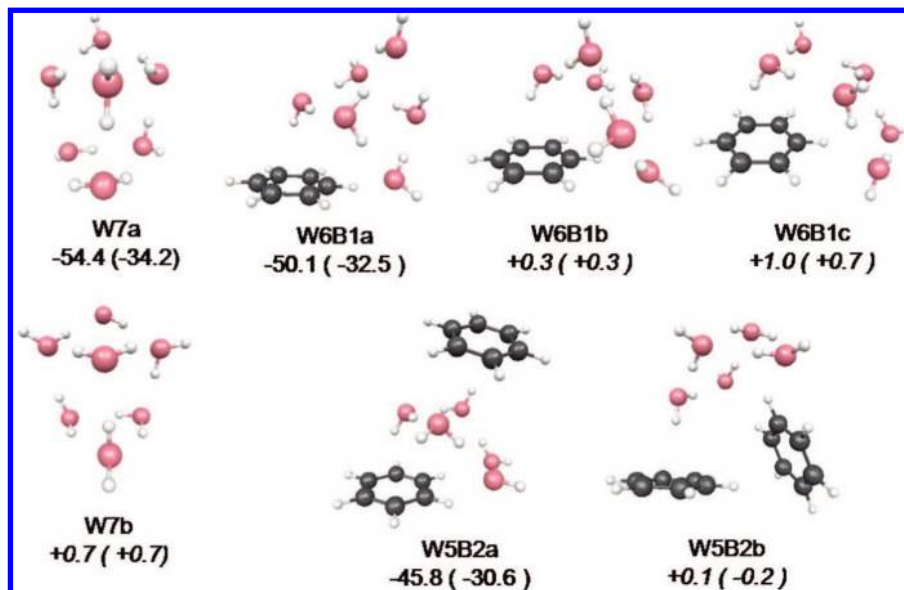


Figure 8. EFP structures of heptamers. See Figure 3 for notations.

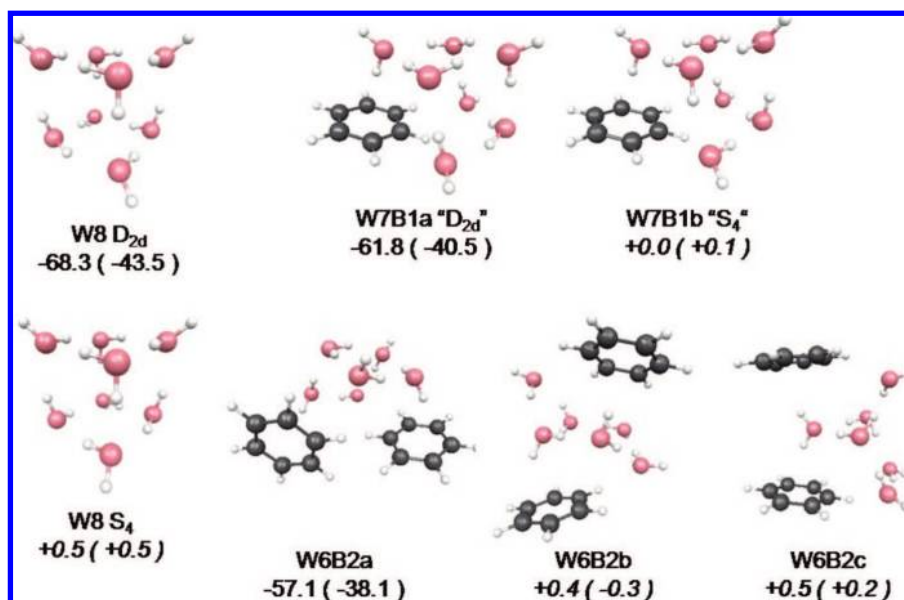


Figure 9. EFP structures of octamers. See Figure 3 for notations.

MP2 and CCSD(T) binding energies for W1B1b are summarized in Table 3. The MP2 and CCSD(T) binding energies for this complex are almost identical. With the aug'cc-pVTZ basis set, the predicted binding energies range from 1.6 kcal/mol (non-BSE corrected) to about 1.2 kcal/mol (CP-corrected), with the average being 1.4 kcal/mol. This is smaller than the EFP binding energy by more than 1 kcal/mol. This difference may be due in part to the use of single point MP2 and CCSD(T) energies. Full optimization of the dimers at these levels of theory could only increase the corresponding binding energies, bringing them into closer agreement with the EFP values. However, the relative energy difference between W1B1a and W1B1b is accurately represented by EFP. EFP puts the W1B1b dimer 1.3 kcal/mol higher in energy, compared with 1.6 kcal/mol for CCSD(T).

All low energy trimers (Figure 4) have triangular structures. In W2B1, benzene serves as a hydrogen bond donor for one water and as an acceptor for the other water. The EFP three-body contributions to the total binding energy in W2B1 are 0.8 kcal/mol versus 1.5 kcal/mol in W3.

The three-body terms in EFP appear to be due to nonadditive polarization interactions. EFP three-body terms for water trimer (-1.5 kcal/mol) compare favorably to the HF 3-body terms (-1.4 kcal/mol). Xantheas found that the presence of correlation in the calculation increases the three-body (and, generally, many body) contributions. For example, for water trimer MP2 three-body contributions are -2.3 kcal/mol compared with the HF value of -1.4 kcal/mol.⁵⁹ However, Jordan and co-workers⁶⁰ found that at least for water hexamers, many-body energies are dominated by Hartree–Fock, while correlation effects are artificial and arise due to incompleteness of the basis set. This seems reasonable since the induction (polarization) forces which provide the major contribution to the many-body effects are rather insensitive to inclusion of correlation. In any case, at least qualitatively, EFP predicts correct values for three-body and many body terms. The significant three-body energy in W2B1 suggests that the polarization forces are enhanced in this complex. In the lowest energy two-benzene–one-water trimer, W1B2a, the water molecule is an H donor in one hydrogen bond to the upper benzene and an H acceptor from the lower benzene.

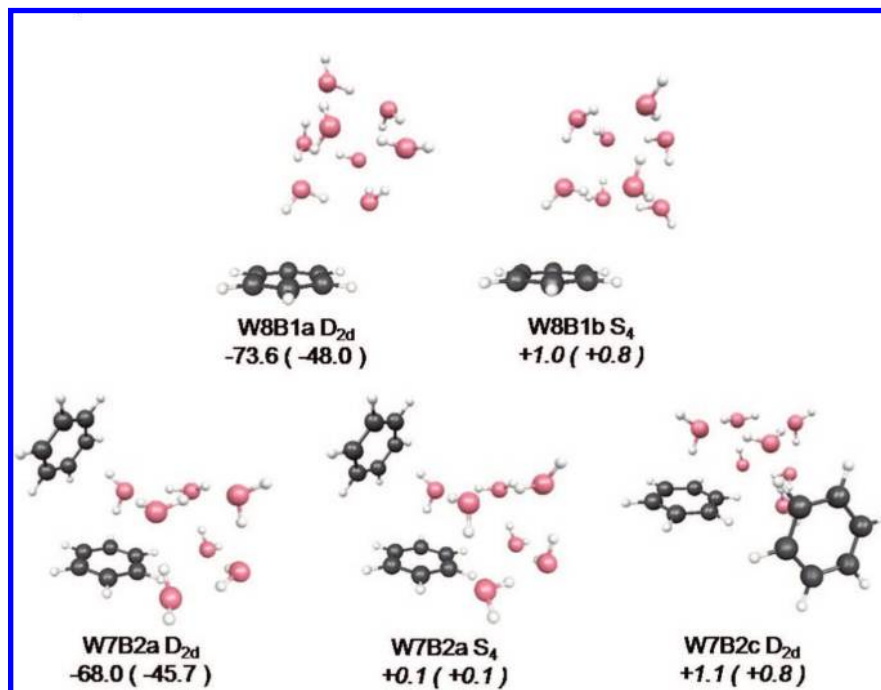


Figure 10. EFP structures of nanomers. See Figure 3 for notations.

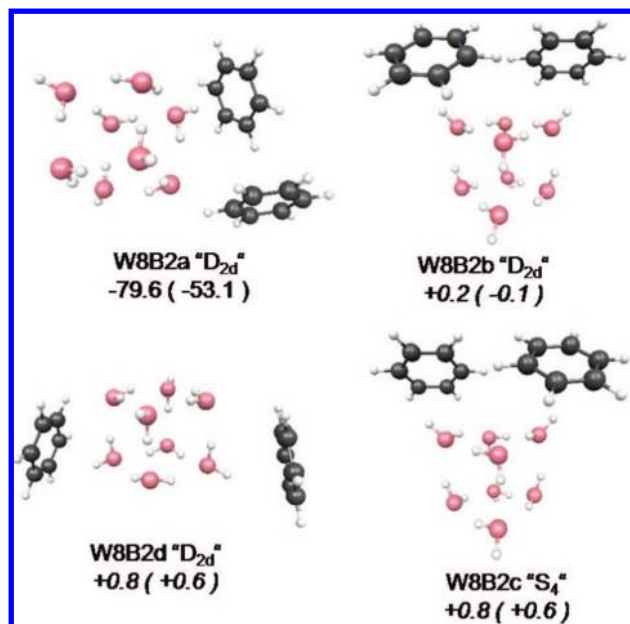


Figure 11. EFP structures of decamers. See Figure 3 for notations.

In the same structure the two benzenes interact with each other in a T-shaped manner. There is a small (-0.4 kcal/mol) collective 3-body affect in this complex. Contrarily, in W1B2b, water is a double H donor, one to each benzene, the polarization cycle is broken, and the resulting three-body term ($+0.5$ kcal/mol !) destabilizes the complex. Due to the unfavorable three-body interactions, this structure is more than 1 kcal/mol higher in energy at the EFP level.

The EFP interaction energies in W2B1 and W1B2a complexes are in good agreement with the MP2 and CCSD(T) energies (see Table 3). As for the dimers, EFP slightly overestimates binding in these complexes (by ~ 1 kcal/mol relative to the average of the CP-corrected and noncorrected CCSD(T) values). It is interesting that EFP is in the best agreement with the noncorrected CCSD(T)/aug'-cc-pVTZ results.

Now, consider the tetramers shown in Figure 5. There is a balance between stronger water–benzene interactions and many-body terms in W3B1a vs a more favorable structure of the water cluster in W3B1b and W3B1c (see Figure 5). The many-body effects in tetramers are defined as three-body plus four-body terms, which are also shown in Figure 5. In agreement with previous findings for water clusters,⁵⁹ the four-body affects constitute about 10% of the total many-body affects. However, depending on the structure, the four-body terms can be either favorable or, as in the case of W3B1b, unfavorable.

W3B1a is the EFP global minimum. However, experimental IR spectra suggest that the observed tetramer has a structure similar to W3B1b, with an approximately cyclic water trimer.^{6,11} The slightly higher energy W3B1c structure exhibits a different orientation of one hydrogen in the water trimer. MP2 and CCSD(T) calculations at the EFP geometries suggest that the W3B1b structure is the global minimum, in agreement with experiment. It is interesting that at the MP2 optimized geometries, the energy differences among the three structures become very small, and the ZPE corrections decrease these differences even further, to only 0.2 kcal/mol (see Table 4). EFP may overestimate the binding in W3B1a because it overbinds the benzene-donor/water-acceptor type bond, as was shown for W1B1b. Nonetheless, the energy differences are very small, as are the differences among the methods.

The three W2B2 tetramers shown in Figure 5 have interesting morphologies. In the lowest energy W2B2a structure, a water dimer interacts favorably with the T-shaped benzene dimer through one donor and one acceptor water–benzene bond. In W2B2b, there are 4 water–benzene bonds, two of each type, and a benzene–benzene parallel slipped-like interaction, but no significant water–water interaction. The benzenes are completely separated in W2B2c, but a water dimer interacts with the benzenes in a manner that is similar to W2B1; that is, with one donor and one weak acceptor hydrogen bond. Complexes a and b are cyclic, and they experience significant many-body effects, -1.9 and -2.0 kcal/mol, respectively, as compared to -4.7 kcal/mol in W4. On the other hand, cooperative forces in

W2B2c are much smaller (-0.6 kcal/mol) and largely responsible for the overall higher energy of this structure. Comparing the EFP and *ab initio* data for the W2B2 complexes (see Table 5), it is apparent that EFP overstabilizes the W2B2b structure. Again, this is probably due to overbinding the benzene-donor water-acceptor intermolecular interaction. In general, the EFP binding energies in W2B2 and W3B1 complexes are $\sim 2-3$ kcal/mol larger than the averaged CP-corrected and noncorrected CCSD(T) values. This is an effect of overstabilization of several water-benzene bonds.

Table 6 provides the EFP interaction energy decomposition in terms of Coulomb, induction, dispersion, and exchange-repulsion terms for water-benzene trimers and tetramers. All four contributing terms play a significant role in the binding and structures of the water-benzene clusters. While the Coulomb term dominates in most of the complexes, the importance of dispersion increases with the number of benzene molecules. Moreover, since the Coulomb term is largely canceled by the exchange-repulsion, the relative isomer energies may be determined by a competition between the induction and dispersion contributions. Similar trends are expected in larger water-benzene complexes.

In pentamers containing one benzene (Figure 6), there is again a competition between the tendency of the water cluster to preserve its cyclic form (i.e., in W4 or W5) and the disturbance of the optimal water tetramer in order to have stronger water-benzene interactions. On the basis of the smaller clusters discussed above, it is likely that the many-body effects stabilize the structures with the benzene built into the water clusters (e.g., W4B1c). Thus, the water tetramer is almost unchanged in W4B1a, whereas the position of one of the hydrogens is modified in W4B1b to allow this water to be an acceptor in a hydrogen bond with benzene. These two conformers have almost identical binding energies, and the relative order is changed by the ZPEs. Because these complexes have many low-frequency modes, the order might change again if one employed the vibrational self-consistent field method⁶¹⁻⁶⁶ to compute the anharmonic vibrational spectrum. The third isomer, W4B1c, has the benzene built into the water ring; i.e., the structure of the original 4-member water ring is strongly disturbed.

In pentamers with two benzenes, the benzenes are separated by a water cluster. W3B2a is almost symmetric along the plane of the water complex, such that each water interacts in a similar manner with both benzenes. For example, one water in W3B2a is a double donor, whereas the other is a double acceptor. The second pentamer, W3B2b, has a cyclic water trimer, with different waters acting as donors to different benzenes. The binding strength per molecule in the water pentamer is weaker than that in the tetramer. That is, the 4-member water ring is more stable than the 5-member ring. Interestingly, this is also true for the benzene-containing complexes; i.e., the differential binding energy of benzene in a tetramer is larger than that in the corresponding pentamer.

Water hexamers are the smallest water clusters with a 3D structure (Figure 7). The lowest energy hexamer isomers are a prism, a cage, and a book, with cyclic and boat-like structures slightly higher in energy. In the two lowest 1-benzene (B1) hexamers, W5B1a preserves the morphology of the 5-member water ring, even though the ring becomes slightly bent. However, W5B1b has a different binding pattern: the water cluster has a cage rather than a ring shape, and the benzene interacts favorably with two waters. Indeed, W5B1b could be considered as a prism structure, with one water substituted by a benzene. As will be shown in additional examples below, the clusters often preserve the morphology of the original water

complex, but with a water-benzene substitution appearing to provide the most stable and compact structures. In the W4B2 clusters, there is an interesting competition between the compact benzene-dimer structure with a preserved 4-member water ring in W4B2a vs the more favorable water-benzene interactions in W4B2b. It seems that the latter interactions become more important when including ZPEs. Interestingly, W4B2a could also be thought of as a book-type cluster with a pair of waters being substituted with two benzenes.

Water heptamers (Figure 8) are less well studied than other water complexes such as hexamers or octamers. In general, they can be seen as hexamers with an extra inserted water molecule or water octamers with one removed water. Depending on the type of excluded water molecule, e.g., double donor-single acceptor (DDA), or single donor-double acceptor (DAA), one could end up with different W7 isomers. Consistent with previous studies,⁶⁷ the two lowest W7 structures predicted by EFP are those obtained from S_4 cubic water octamers by exclusion of DDA (W7a) and DAA (W7b) waters (see Figure 8).

Water heptamers consist of a combination of one 3-member, three 4-member, and one 5-member ring. Clusters with one benzene have well defined substructures of water hexamers; these are a cage in W6B1a and books in W6B1b and W6B1c. W6B1a may be considered as a water heptamer W7a with one water molecule substituted by a benzene. The two lowest-energy conformers of clusters with two benzenes are almost isoenergetic. In W5B2a, the benzenes are separated by the water complex, whereas in W5B2b the benzenes are together in a T-shaped configuration. Strikingly, the morphology of W5B2b is also similar to that of W7a.

Two lower energy water octamers, compact cubic complexes, differ in the orientation of their hydrogen bonds (Figure 9). In the global minimum (approximately) D_{2d} isomer, the hydrogen bonds of the top and bottom faces of the cube are oriented in opposite directions, whereas the hydrogen bonds are oriented in the same direction in the S_4 isomer. When one water is substituted with a benzene, benzene builds into the water cube without any significant disturbance of the water network. Similarly to pure water octamers, W7B1 complexes can be distinguished by the orientation of hydrogen bonds, and the " D_{2d} " isomer (W7B1a), with opposite directions of the hydrogen bonding cycles, is lower in energy. The first two octamers with two benzenes also originate from the cubic water cluster. However, in both cases, the large size of the benzene rings results in significant distortions. As in the case of the 2-benzene heptamers, the structures with both close and separated benzenes are very similar in energy and their order changes by including ZPEs. Due to the compact structure and the strong hydrogen bonding network, the effective binding energies per molecule in the octamers are higher than those in the hexamers and heptamers. Again, this is true for both the pure water and water-benzene clusters.

In clusters with one benzene and eight waters (Figure 10), benzene does not destroy the stable cubic structure of water but simply attaches to one of the dangling OH bonds. The two lowest-energy structures are obtained by combining benzene with D_{2d} and S_4 types of cubes, with the D_{2d} -like cube being lower in energy. For the two-benzene clusters, the lowest-energy structures are deduced by adding the second benzene to compact W7B1 complexes. It is not surprising that the distinct " D_{2d} "-like and " S_4 "-like structures are present here too, with the former again being the lower in energy. The most favorable position

of the second benzene is in proximity to the first one, such that both benzenes are connected to the same water molecule.

Finally, the W8B2 complexes are shown in Figure 11. Similar to the W8B1 clusters, the cubic water structure stays unchanged. Structures with S_4 -like cubes are higher in energy. The EFP results suggest that benzenes are either connected to neighboring dangling OH bonds and interact slightly with each other (W8B2b), or they are T-shaped and organize a hydrogen bonding cycle with one of the edges of the water cube (W8B2a).

IV. Conclusions

This paper presents a study of (water)_{1–8}–(benzene)_{1–2} complexes based on the general effective fragment potential (EFP) method. The lowest energy conformers for each of the considered clusters were found by using the Monte-Carlo technique. In order to benchmark the accuracy of the EFP approach, binding energies in the smallest clusters were also evaluated at the MP2 and CCSD(T) levels of theory.

An interesting finding of this study is that in small water–benzene complexes, benzene is revealed to be both a donor and an acceptor of a hydrogen bond. Benzene is polarizable and participates in hydrogen bonding networking and within the cooperative behavior of water clusters. Often, benzene can substitute for a water molecule without destroying the morphology of a water cluster. Since the water–benzene interactions are only slightly weaker than the water–water interactions, there is often a competition between structures with different numbers of water–water, benzene–water, and benzene–benzene hydrogen bonds. Because energy differences between isomers are small, the present analysis does not provide a clear answer to whether, in clusters with two benzenes, the benzene rings prefer to separate from each other and interact mainly with water molecules, or prefer to remain close enough to each other to maintain direct π – π interactions. In several complexes considered in this work, structures of both types occur with only minor and inconclusive energy differences. However, in the largest 7-water and 8-water complexes, benzenes prefer to stay in proximity to one another, possibly driven by the analogous propensity for water molecules.

In general, EFP accurately predicts structures and binding energies in the water–benzene complexes. However, some slight discrepancies in the relative order of binding energies are observed. This can be explained by the tendency of EFP to overestimate the binding in the benzene-donor–water-acceptor configuration. However, taking into account the complicated nature of the interactions between water and benzene and the small energy differences between different structures, the accuracy of EFP is still very reasonable.

Interactions between aromatic molecules and solvents are fundamental in biology. The focus of this effort has been on the simplest of these systems, the water–benzene complexes. Future work will analyze extended systems such as described in ref 68 and problems related to biochemistry, such as the interactions between DNA base pairs and different solvents.

Acknowledgment. This work was supported in part by a Department of Energy SciDAC grant to the Ames Laboratory (MSG), and in part by a NIRT grant from the National Science Foundation (LVS).

Supporting Information Available: Text file giving the EFP and MP2 geometries of water–benzene clusters. This material is available free of charge via the Internet at <http://pubs.acs.org>.

References and Notes

- (1) Atwood, J. L.; Hamada, F.; Robinson, K. D.; Orr, G. W.; Vincent, R. L. *Nature* **1991**, *349*, 683.
- (2) Hummer, G.; Rasaiah, J. C.; Noworyta, J. P. *Nature* **2001**, *414*, 188.
- (3) Meyer, E. A.; Castellano, R. K.; Diederich, F. *Angew. Chem., Int. Ed.* **2003**, *42*, 1210.
- (4) Scheraga, H. A.; Khalili, M.; Liwo, A. *Annu. Rev. Phys. Chem.* **2007**, *58*, 57.
- (5) Feller, D. *J. Phys. Chem. A* **1999**, *103*, 7558.
- (6) Fredericks, S. Y.; Pedulla, J. M.; Jordan, K. D.; Zwier, T. S. *Theor. Chem. Acc.* **1997**, *96*, 51.
- (7) Gotch, A. J.; Zwier, T. S. *J. Chem. Phys.* **1992**, *96*, 3388.
- (8) Gruenloh, C. J.; Carney, J. R.; Arrington, C. A.; Zwier, T. S.; Fredericks, S. Y.; Jordan, K. D. *Science* **1997**, *276*, 1678.
- (9) Gruenloh, C. J.; Carney, J. R.; Hagemester, F. C.; Arrington, C. A.; Zwier, T. S.; Fredericks, S. Y.; Wood, J. T.; Jordan, K. D. *J. Chem. Phys.* **1998**, *109*, 6601.
- (10) Pribble, R. N.; Garrett, A. W.; Haber, K.; Zwier, T. S. *J. Chem. Phys.* **1995**, *103*, 531.
- (11) Pribble, R. N.; Zwier, T. S. *Science* **1994**, *265*, 75.
- (12) Pribble, R. N.; Zwier, T. S. *Faraday Discuss.* **1994**, 229.
- (13) Tarakeshwar, P.; Choi, H. S.; Lee, S. J.; Lee, J. Y.; Kim, K. S.; Ha, T. K.; Jang, J. H.; Lee, J. G.; Lee, H. *J. Chem. Phys.* **1999**, *111*, 5838.
- (14) Tsuzuki, S.; Honda, K.; Uchimaru, T.; Mikami, M.; Tanabe, K. *J. Am. Chem. Soc.* **2000**, *122*, 11450.
- (15) Baron, M.; Kowalewski, V. J. *J. Phys. Chem. A* **2006**, *110*, 7122.
- (16) Cheng, B. M.; Grover, J. R.; Walters, E. A. *Chem. Phys. Lett.* **1995**, *232*, 364.
- (17) Courty, A.; Mons, M.; Dimicoli, N.; Piuze, F.; Gageot, M. P.; Brenner, V.; de Pujo, P.; Millie, P. *J. Phys. Chem. A* **1998**, *102*, 6590.
- (18) Gutowsky, H. S.; Emilsson, T.; Arunan, E. *J. Chem. Phys.* **1993**, *99*, 4883.
- (19) Jedlovszky, P.; Kereszturi, A.; Horvai, G. *Faraday Discuss.* **2005**, *129*, 35.
- (20) Suzuki, S.; Green, P. G.; Bumgarner, R. E.; Dasgupta, S.; Goddard, W. A.; Blake, G. A. *Science* **1992**, *257*, 942.
- (21) Moller, C.; Plesset, S. *Phys. Rev.* **1934**, *46*, 618.
- (22) Gordon, M. S.; Slipchenko, L. V.; Li, H.; Jensen, J. H. *Ann. Rep. Comput. Chem.* **2007**, *3*, 177.
- (23) Chen, W.; Gordon, M. S. *J. Chem. Phys.* **1996**, *105*, 11081.
- (24) Webb, S. P.; Gordon, M. S. *J. Phys. Chem. A* **1999**, *103*, 1265.
- (25) Adamovic, I.; Gordon, M. S. *J. Phys. Chem. A* **2006**, *110*, 10267.
- (26) Slipchenko, L. V.; Gordon, M. S. *J. Comput. Chem.* **2007**, *28*, 276.
- (27) Smith, T.; Slipchenko, L. V.; Gordon, M. S. *J. Phys. Chem.* 2008, in press.
- (28) Raghavachari, K.; Trucks, G. W.; Pople, J. A.; Head-Gordon, M. *Chem. Phys. Lett.* **1989**, *157*, 479.
- (29) Schmidt, M. W.; Baldridge, K. K.; Boatz, J. A.; Elbert, S. T.; Gordon, M. S.; Jensen, J. H.; Koseki, S.; Matsunaga, N.; Nguyen, K. A.; Su, S. J.; Windus, T. L.; Dupuis, M.; Montgomery, J. A. *J. Comput. Chem.* **1993**, *14*, 1347.
- (30) Gordon, M. S.; Schmidt, M. W. In *Theory and Applications of Computational Chemistry*; Dykstra, C. E., Frenking, G., Kim, K. S., Scuseria, G. E., Eds.; Elsevier: Amsterdam, 2005; Chapter 41.
- (31) Stone, A. J. *The Theory of Intermolecular Forces*; Oxford University Press: Oxford, U.K., 1996.
- (32) Jensen, J. H.; Gordon, M. S. *Mol. Phys.* **1996**, *89*, 1313.
- (33) Hehre, W. J.; Ditchfield, R.; Pople, J. A. *J. Chem. Phys.* **1972**, *56*, 2257.
- (34) Adamovic, I.; Gordon, M. S. *Mol. Phys.* **2005**, *103*, 379.
- (35) Amos, R. D.; Handy, N. C.; Knowles, P. J.; Rice, J. E.; Stone, A. J. *J. Phys. Chem.* **1985**, *89*, 2186.
- (36) Li, H.; Gordon, M. S.; Jensen, J. H. *J. Chem. Phys.* **2006**, *124*.
- (37) Krishnan, R.; Binkley, J. S.; Seeger, R.; Pople, J. A. *J. Chem. Phys.* **1980**, *72*, 650.
- (38) Clark, T.; Chandrasekhar, J.; Spitznagel, G. W.; Schleyer, P. V. *J. Comput. Chem.* **1983**, *4*, 294.
- (39) Frisch, M. J.; Pople, J. A.; Binkley, J. S. *J. Chem. Phys.* **1984**, *80*, 3265.
- (40) Dunning, T. H. *J. Chem. Phys.* **1989**, *90*, 1007.
- (41) Kendall, R. A.; Dunning, T. H.; Harrison, R. J. *J. Chem. Phys.* **1992**, *96*, 6796.
- (42) Sinnokrot, M. O.; Valeev, E. F.; Sherrill, C. D. *J. Am. Chem. Soc.* **2002**, *124*, 10887.
- (43) Gordon, M. S.; Freitag, M. A.; Bandyopadhyay, P.; Jensen, J. H.; Kairys, V.; Stevens, W. J. *J. Phys. Chem. A* **2001**, *105*, 293.
- (44) Slipchenko, L. V.; Gordon, M. S. Unpublished results.
- (45) Day, P. N.; Pachter, R.; Gordon, M. S.; Merrill, G. N. *J. Chem. Phys.* **2000**, *112*, 2063.
- (46) McKee, M. L.; Lipscomb, W. N. *J. Am. Chem. Soc.* **1981**, *103*, 4673.

- (47) Pople, J. A.; Head-Gordon, M.; Fox, D. J.; Raghavachari, K.; Curtiss, L. A. *J. Chem. Phys.* **1989**, *90*, 5622.
- (48) Curtiss, L. A.; Raghavachari, K.; Trucks, G. W.; Pople, J. A. *J. Chem. Phys.* **1991**, *94*, 7221.
- (49) Curtiss, L. A.; Raghavachari, K.; Redfern, P. C.; Rassolov, V.; Pople, J. A. *J. Chem. Phys.* **1998**, *109*, 7764.
- (50) Bytautas, L.; Ruedenberg, K. *J. Chem. Phys.* **2005**, 122.
- (51) Halkier, A.; Helgaker, T.; Jorgensen, P.; Klopper, W.; Koch, H.; Olsen, J.; Wilson, A. K. *Chem. Phys. Lett.* **1998**, *286*, 243.
- (52) Jensen, F. *Theor. Chem. Acc.* **2000**, *104*, 484.
- (53) Kutzelnigg, W. *Int. J. Quantum Chem.* **1994**, *51*, 447.
- (54) Kutzelnigg, W.; Morgan, J. D. *J. Chem. Phys.* **1992**, *96*, 4484.
- (55) Truhlar has previously noted that CP-corrected interaction energies often over-correct by as much as the original BSSE error (Schwenke, D. W.; Truhlar, D. G. *J. Chem. Phys.* **1985**, *82*, 2418).
- (56) Hill, A. E. *J. Am. Chem. Soc.* **1922**, *44*, 1163.
- (57) Alexander, D. M. *J. Phys. Chem.* **1959**, *63*, 1021.
- (58) Polak, J.; Lu, B. C. Y. *Can. J. Chem.—Rev. Can. Chim.* **1973**, *51*, 4018.
- (59) Xantheas, S. S. *J. Chem. Phys.* **1994**, *100*, 7523.
- (60) Pedulla, J. M.; Kim, K.; Jordan, K. D. *Chem. Phys. Lett.* **1998**, *291*, 78.
- (61) Bowman, J. M. *J. Chem. Phys.* **1978**, *68*, 608.
- (62) Chaban, G. M.; Jung, J. O.; Gerber, R. B. *J. Chem. Phys.* **1999**, *111*, 1823.
- (63) Cohen, M.; Greita, S.; Mceachran, R. P. *Chem. Phys. Lett.* **1979**, *60*, 445.
- (64) Gerber, R. B.; Ratner, M. A. *Chem. Phys. Lett.* **1979**, *68*, 195.
- (65) Njegic, B.; Gordon, M. S. *J. Chem. Phys.* **2006**, 125.
- (66) Yagi, K.; Hirao, K.; Taketsugu, T.; Schmidt, M. W.; Gordon, M. S. *J. Chem. Phys.* **2004**, *121*, 1383.
- (67) Kim, J.; Majumdar, D.; Lee, H. M.; Kim, K. S. *J. Chem. Phys.* **1999**, *110*, 9128.
- (68) Tauer, T. P.; Sherrill, C. D. *J. Phys. Chem. A* **2005**, *109*, 10475.

JP808845B